SPE 162673

An Investigation of Vertical and Lateral Communication in an Unconventional Oil Reservoir Using Geochemistry and Reservoir Simulation

Faisal Rasdi, Ahmad Salman, Doyle A. Adams, Zvi Sofer, Marathon Oil Corporation

This paper was prepared for presentation at the SPE Canadian Unconventional Resources Conference held in Calgary, Alberta, Canada, 30 October–1 November 2012.

Abstract

Vertical and horizontal inter-well communication in unconventional reservoirs remains a major uncertainty. This paper presents the results of geochemical analyses performed on several wells in the Bakken and Three Forks unconventional oil reservoirs. Geochemical analyses performed on oil extracted from core, oil sampled while drilling, and oil produced after stimulation indicate that the geochemical signatures of the Bakken and Three Forks Formations are different and unique to its respective stratigraphic units. Using unique geochemical signatures, this study developed a procedure for identifying the production of mixed oils and the relative contribution from each contributing startigraphic units.

To further investigate vertical communication a detailed geologic model was constructed using core and outcrop data. The model was simulated and history matched to estimate contribution from adjacent layers. Various scenarios were simulated to understand the probability of communication. Analyses suggest that vertically adjacent layers contribute to production as predicted by the reservoir model and measured by the geochemical signature of the oil.

This paper demonstrates (a) contribution from vertically adjacent formations can be significant, (b) geochemistry may be utilized to quantify vertical drainage, and (c) quantification of contribution from offset layers helped to constrain a reservoir simulation history match. Results from this study have facilitated the assessment of the degree of vertical communication across various flow units, which is the key to an efficient reservoir development.

Introduction

Unconventional reservoirs present unique challenges to understanding reservoir performance and communication, primarily because of very low permeability and complex wellbore geometry. These reservoirs require stimulation by hydraulic fracturing treatment and a large infill well drilling program to be economical. Cipolla et al. (2010, 2011) suggests that the productivity and drainage of an unconventional well is mostly controlled by the effectiveness of the hydraulic fracture treatment. Additionally, a study by Mullen et al. (2010) supports and implies that the existing natural fractures are also a critical component of unconventional reservoirs. This paper evaluates the drainage and communication created by the hydraulic fracture treatment and the existing natural fracture networks.

This study focuses on the development of the Bakken Petroleum System, comprised of multiple unconventional reservoirs in the Williston Basin. The reservoir contains fine grained sandstone and silty dolostone within a middle member, which is bounded by organic rich shales (Upper and Lower Bakken) that are both sources and seals (Pitman et al. 2010). **Fig. 1** displays the typical stratigraphic logs for the Bakken system. The United States Geological Survey estimates the mean technologically recoverable resource for the Bakken Formation to be 3.65 Bbbls of Oil, 1.85 Tcf of associated/dissolved natural gas, and 148 MMBLs of natural gas liquids (USGS, 2008), making the Bakken Play one of the biggest oil fields in the United States.

Microseismic studies espoused by Cipolla et al. (2010, 2011) and Warpinski et al. (2008) suggest that hydraulic fracturing treatment creates a complex fracture network, which is commonly referred to as stimulated reservoir volume (SRV). SRV enables the well to connect and produce aerially and vertically to the adjoining layers. This study utilizes geochemistry to understand the communication between the bounding layers of the Bakken. This understanding is crucial in optimizing the number of wells, especially when the development involves producing Middle Bakken and Three Forks, which are on average only 45 vertical-feet apart.

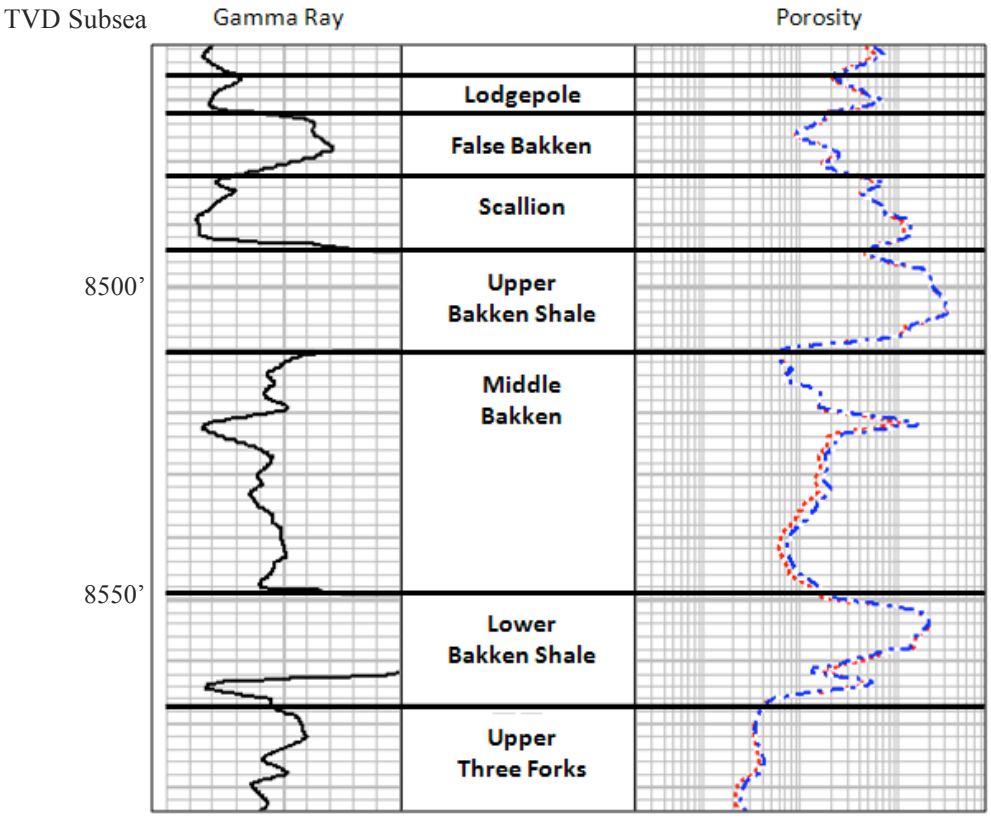

Fig. 1— Stratigraphic type log of the five horizons of interest, which include the Lower Lodgepole, Upper Bakken Shale, Middle Bakken, Lower Bakken Shale and Upper Three Forks

Geochemistry in this study involves analyzing isotopic signatures. This paper utilizes the geochemistry-production allocation technique proposed by McCaffrey et al. (1996, 2010, 2011, 2012) to differentiate and allocate production from the various geologic members within the Bakken system.

Reservoir models are built for this study to understand the behavior of the reservoir, quantify the reservoir potential and assess the degree of communication. The reservoir models include a detailed fracture network characterization or commonly known as discreet fracture network (DFN) model. The DFN model was later upscaled and converted to a dual porosity model for dynamic simulation. The workscope of the DFN construction will not be discussed here, but the result of utilizing the DFN model will be shared in this paper.

This paper shows how we have integrated geochemistry results and reservoir simulation to gain insights into the pressure and production communication observed in the field. The calibrated reservoir models can later be used to run sensitivities to predict reserves, determine the decline parameters and optimize development plan.

Field Example of Reservoir Communication

Recently a Marathon Oil horizontal well drilled in the Three Forks target zone was hydraulically stimulated and pressured up an adjacent Marathon Oil horizontal well drilled in the Middle Bakken target zone in the process. **Fig. 2a)** shows the type log for Middle Bakken and Three Forks and the respective target zone depths. As shown in **Fig. 2b)**, the wellbores are 648' apart at their closest lateral points and 42' apart at their closest vertical points. **Fig. 3** shows that tubing pressure measured at surface in the Middle Bakken well increased from 75 psi to over 3000 psi during hydraulic stimulation in the adjacent Three Forks well. This suggests that the pressure was translated into the Middle Bakken well during stimulation but does not imply that the Three Forks completion effort effectively stimulated the Middle Bakken reservoir. Marathon Oil has observed numerous field examples similar to this one, which incited the investigation of whether the pressure communication can be translated to production communication.

Ultimately, this study aims to develop a methodology to determine oil allocation from different reservoirs. In the previous example, isotopic signatures from produced oil from the Three Forks well would be used to evaluate whether or not it is also producing oil from the Middle Bakken reservoir.

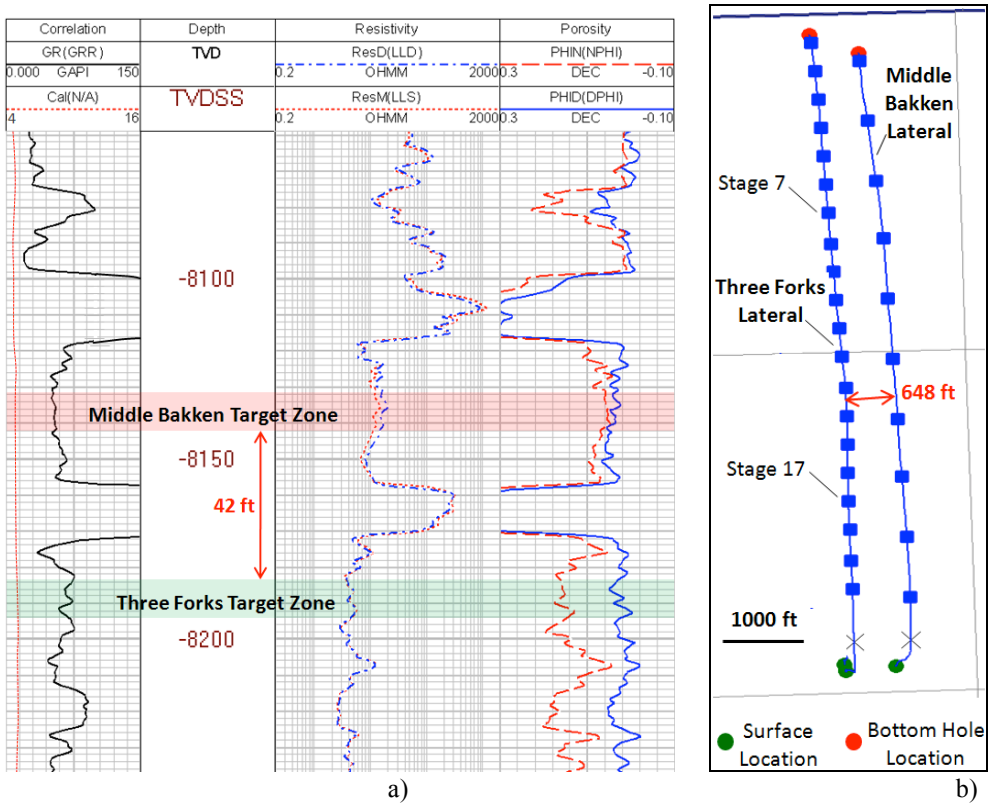

Fig. 2 a) — Type log depicting the Middle Bakken and Three Forks target zones atop gamma ray, resistivity, and porosity curves. The base of Middle Bakken target zone is 42 ft from the top of Three Forks target zone
b) — Map view of the two laterals. They are 648 ft apart at their nearest points

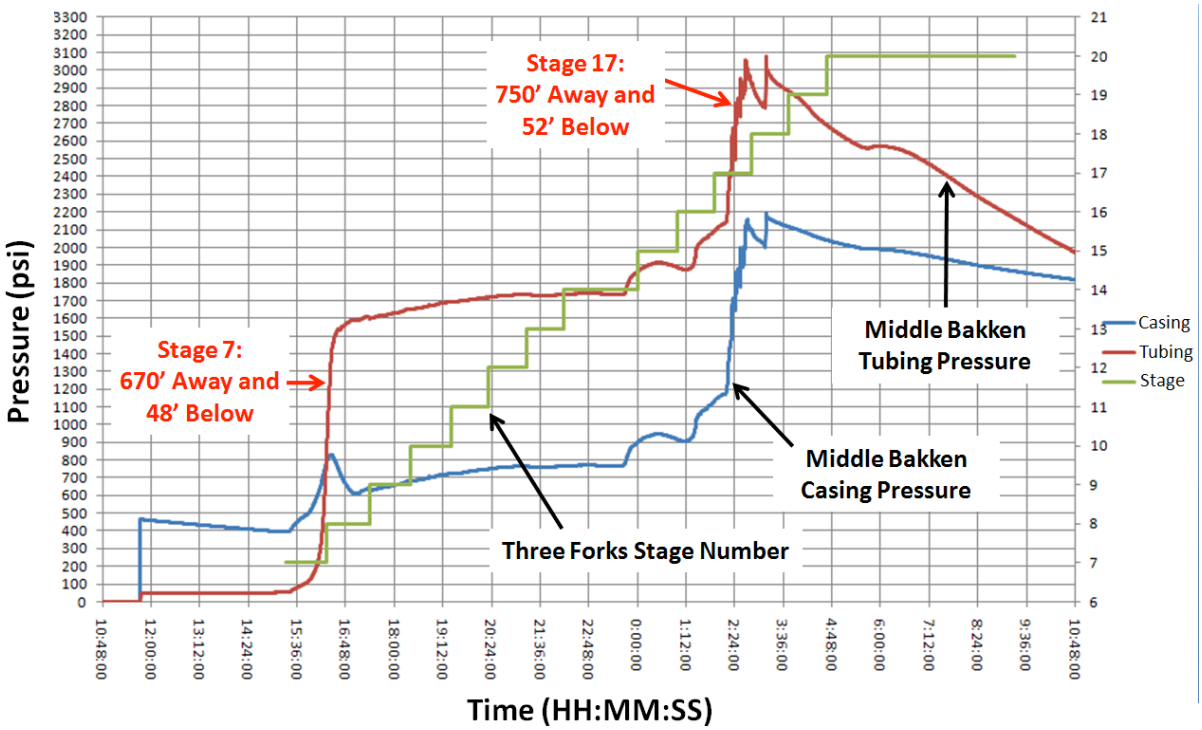

Fig. 3— Surface pressure recorded in the offset Middle Bakken lateral during the hydraulic fracture stimulation in the Three Forks lateral. Note that pressure spikes during completion in stages 7 and 17 with tubing pressures in excess of 3000 psi during stage 17

Isotope Geochemistry: A Brief Review

A sample of oil is often comprised of both hydrocarbons and non-hydrocarbons. Hydrocarbons are subdivided into two groups, saturates and aromatics, based upon their structural formulae. Produced oil will typically contain higher components of saturates and aromatics. Saturates are comprised of carbon-chained molecules and aromatics are cyclical molecules containing one or more carbon rings. Non-hydrocarbons are present in oil in the form of resins (NSOs) and asphaltenes and may also contain nitrogen, oxygen, and sulfur in addition to hydrogen and carbon. Resins are heterocyclic compounds, such as acids, bases, and phenolics, and asphaltenes are larger, less mobile molecules (Bissada et al. 1992).

Carbon-13 (C-13), a naturally occurring carbon isotope, bonds differently in saturates than in aromatics and the energies in these bonds may be recorded as unique chemical signatures. Similarly, carbon in aromatics bond differently than NSOs and asphaltenes so that each fraction of oil may be tested for a unique isotopic signature. These carbon isotope energies, or carbon fixation energies, vary further based upon the thermal history and source material of the oil sampled. Thus, C-13 bonds within a saturate molecule sampled from a deeper part of a basin may likely differ from C-13 bonds measured in a saturate molecule sampled from the fringes of the same basin. This study utilized the ratio of C-13 isotopic signatures to differentiate and ultimately quantify oil from different stratigraphic horizons within the Bakken Petroleum system.

Utilizing Geochemistry for Production Allocation

Identifying unique geochemical signatures to measure and allocate production from multiple producing zones has been utilized in the oil and gas industry for several years (McCaffrey et al. (1996, 2010, 2011, 2012) and Bennett et al. 2009). In order to estimate production contribution from specific stratigraphic zones, end member oil samples as well as produced oil samples must be procured. The five zones of interest that may contribute to hydraulically fractured well production are the Lodgepole, Upper Bakken Shale, Middle Bakken, Lower Bakken Shale and Upper Three Forks units.

For this study, end member oil samples were extracted from vertical core sections taken from all of the five stratigraphic zones of interest in the Bakken petroleum system, and samples were also taken while drilling in target zones. Produced oil samples were collected from wells that were in close proximity to where core samples and samples taken while drilling were collected. Produced oils were sampled at a frequency of once per month. Stable carbon isotope analysis measuring the C-13/C-12 isotopic ratio ($\delta^{13}C$) in the saturate, aromatic, NSO and asphaltene oil fractions as well as the un-fractionated whole oil were performed on both end member and produced oil samples. An example of the results of the stable carbon isotope analysis for the saturate and aromatic fractions taken from vertical core data are shown in **Fig. 4 a) and 5**. Stratigraphic profiles of $\delta^{13}C$ saturate and aromatic values are shown in **Fig. 4 a) and b)**. A cross plot of $\delta^{13}C$ saturate vs. aromatic values illustrates the isotopic differences between each of the five stratigraphic zones can be seen in **Fig. 5**.

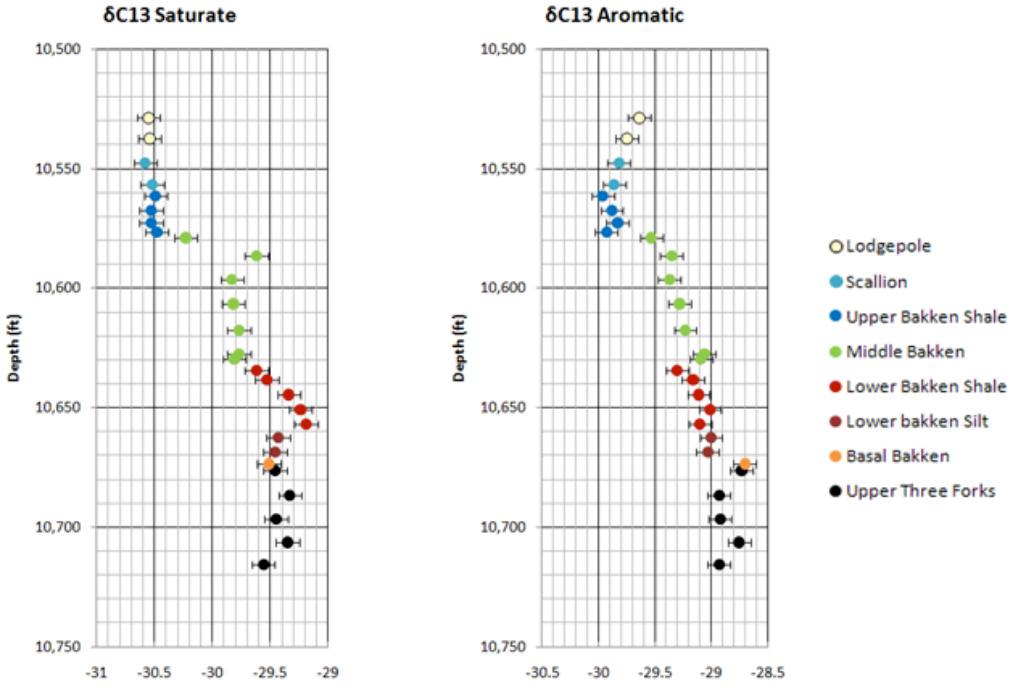

Fig. 4 a) and b) — The charts on the left and right are stratigraphic descriptions of $\delta^{13}C$ saturate and aromatic values, respectively

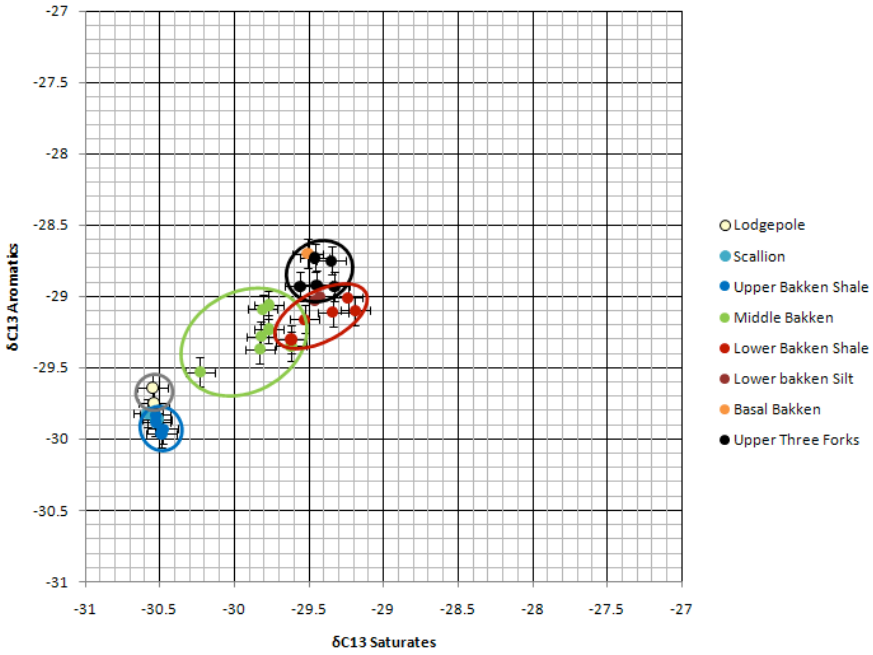

Fig. 5— A cross plot of $\delta^{13}C$ saturate vs. aromatic values. Marked circles identify each of the five stratigraphic zones of interest in this study

Produced oil $\delta^{13}C$ saturate, aromatic, NSO, asphaltene and whole oil values were compared against end member values in order to gauge whether oil production was coming directly from the target zone where a well was drilled and completed in. Produced oil $\delta^{13}C$ values from numerous wells located in close proximity to where end member samples were collected show that contribution from multiple zones occurs throughout the life of the well. Measured and tested produced oil samples taken from a Middle Bakken and Three Forks drilled and completed well can be seen measured against the end member $\delta^{13}C$ isotope values on **Fig. 6**. An idealized diagram depicting what may be occurring throughout the producing life of a hydraulically fractured well is shown in **Fig. 7**.

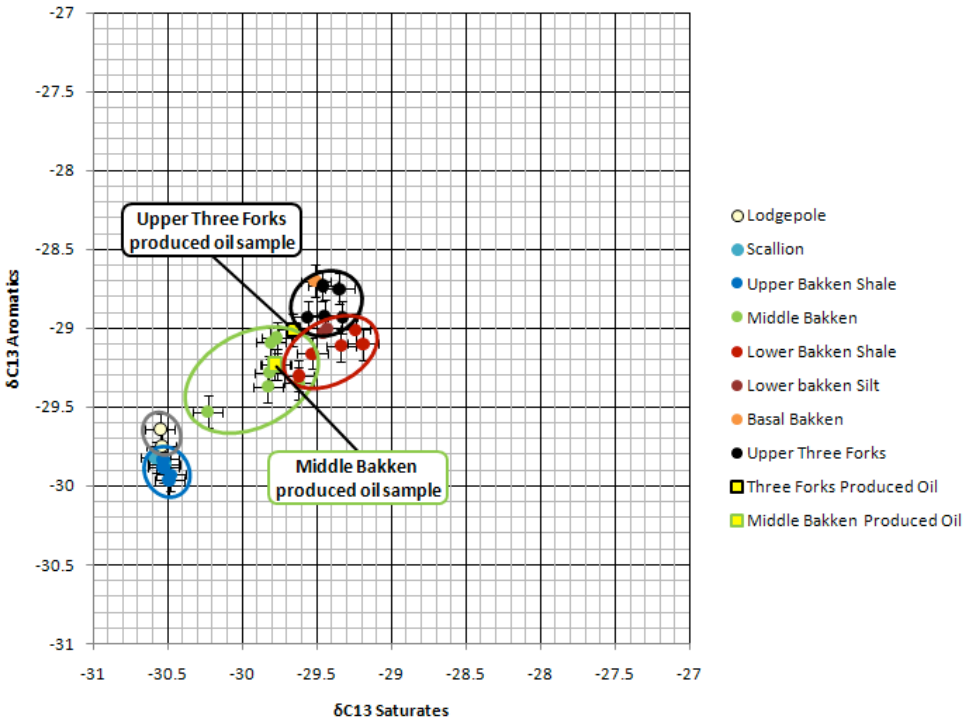

Fig. 6— Cross plot of $\delta^{13}C$ saturate vs. aromatic values. Produced oil values shown to be a mixture of oil from multiple zones

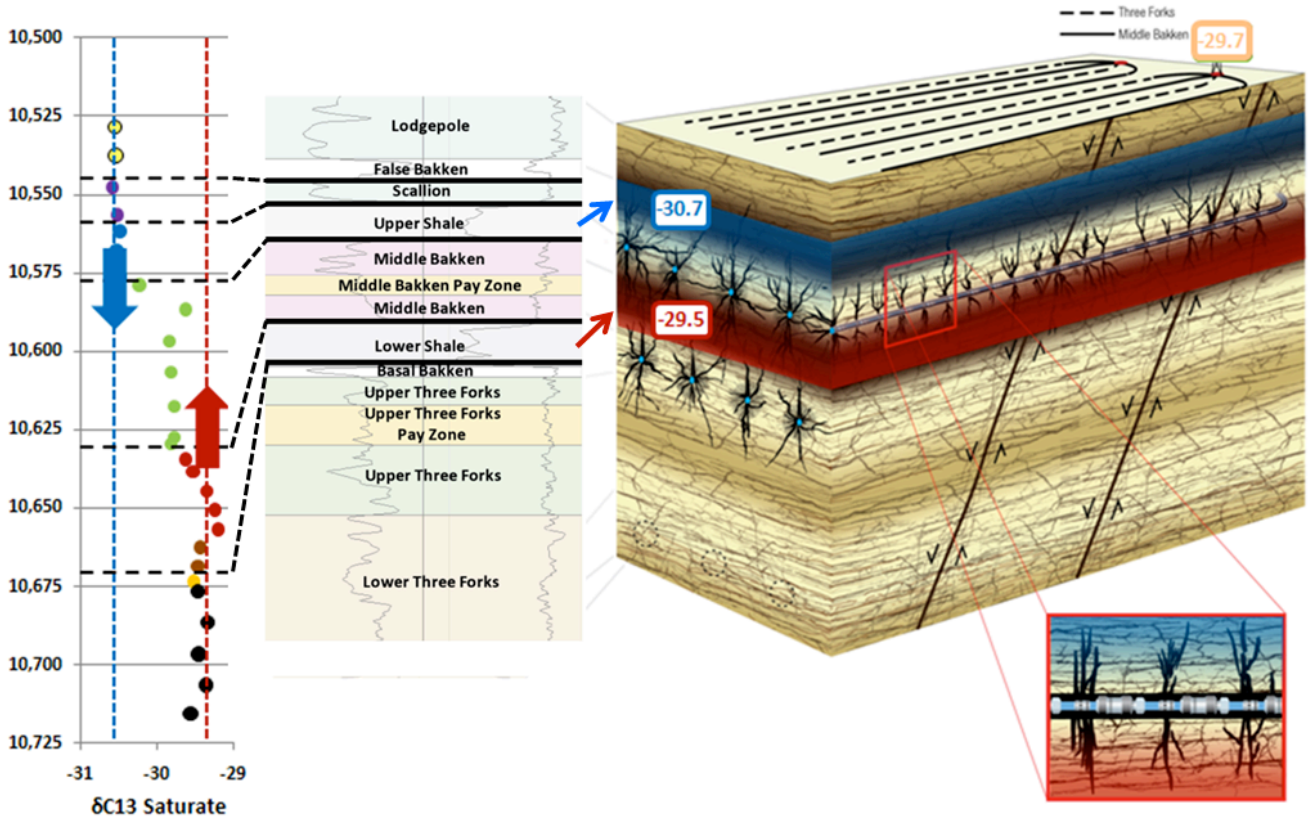

Fig. 7— Idealized depiction of contribution from multiple zones above and below the target zone where a well is drilled and completed

The method proposed by McCaffrey et al. (2010, 2011, 2012) to allocate production from multiple contributing zones utilizing isotopic values was employed to estimate contribution from each of the five zones of interest. The method utilizes the isotopic values for the saturate, aromatic, NSO, asphaltene fractions as well as the un-fractionated whole oil and solves a simultaneous mass balance system of equations. **Appendix A** illustrates in detail an example of the production allocation calculation on a Three Forks producing well.

Results from applying the McCaffrey et al. (2010, 2011, 2012) method of production allocation to the end member and Three Forks produced oil sample data yields a percent contribution of 18% from the Middle Bakken, 27% from the Lower Bakken Shale and 55% from the Upper Three Forks zones. **Fig. 8** shows the production allocation by layers for the Three Forks producing wells. The production allocation results represent percent contribution from specific zones for a single day and not for the entire life of the well. Periodic sampling, analysis and allocation are required to accurately estimate contribution throughout the producing life of the well.

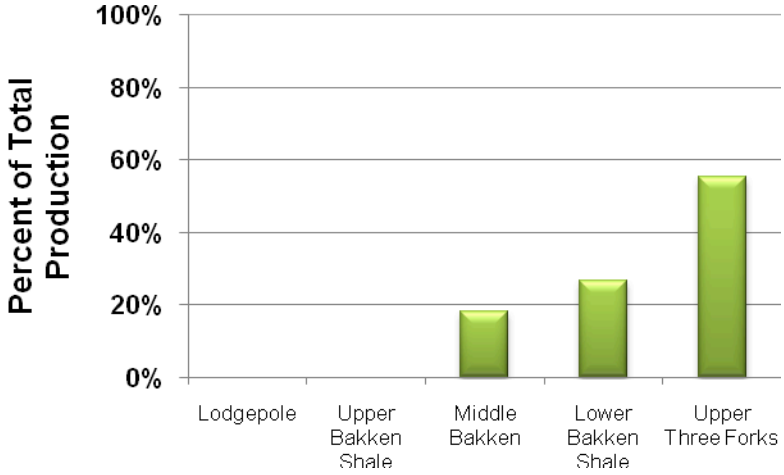

Fig. 8— Production contribution by layers for a Three Forks producer

Integrating Field Data, Geochemistry Results and Numerical Simulation

A numerical reservoir flow simulation was utilized in the study to understand the full potential of the Bakken and evaluate the degree of communication. This section presents an overview of the construction of the geocellular model, an example of a full vertical communication well performance, single layer with vertical barriers well performance, and a calibrated well performance. The decline behavior observed in the models and in the field will also be discussed to provide insight into layer communications, in term of production analysis.

Simulation Model. This paper will not detail the construction of the geocellular model, as that was not the intent of the paper. A suite of data (cores, logs and well testing) are used to characterize the DFN. These data provide high confidence on the location, orientation and property of natural fractures in the system. A similar data integration workflow proposed by Ejofodomi et al. (2011) was utilized in this study.

Various literatures (Mullen et al. 2010, Cipolla et al. 2010, and Rasdi et al. 2012) have advocated the existence of natural fractures to explain the high initial production and rapid decline behavior in the unconventional reservoirs. This paper illustrates the use of Gross et al. (2007) conceptual fracture model to gain insights of production behavior and vertical communication between the layers in the Bakken system. The model includes a characterization of pervasive natural fractures, fault related fractures and fracture corridors. **Fig 9.** shows a tectonic multi scale conceptual fracture model by Gross et al (2007), which was translated into a dual porosity simulation model in **Fig 10**.

Well A is selected for this study. A history matching effort was completed for Well A to gain insight of the history matching parameters. Since Well A only has about 2 years of data, tuning the SRV property is found to be sufficient to match the historical rates and pressure data. **Table 1** shows the completion detail of the well, which was used in the simulation model.

TABLE 1—MODEL PARAMETERS FOR WELL A

Horizontal Well Length, ft	9,000
Number of Stages	15
SRV Permeability, md	0.015
SRV Porosity, %	0.2
Initial Hydraulic Fracture Conductivity, md-ft	116
Fracture Half-Length, ft	200

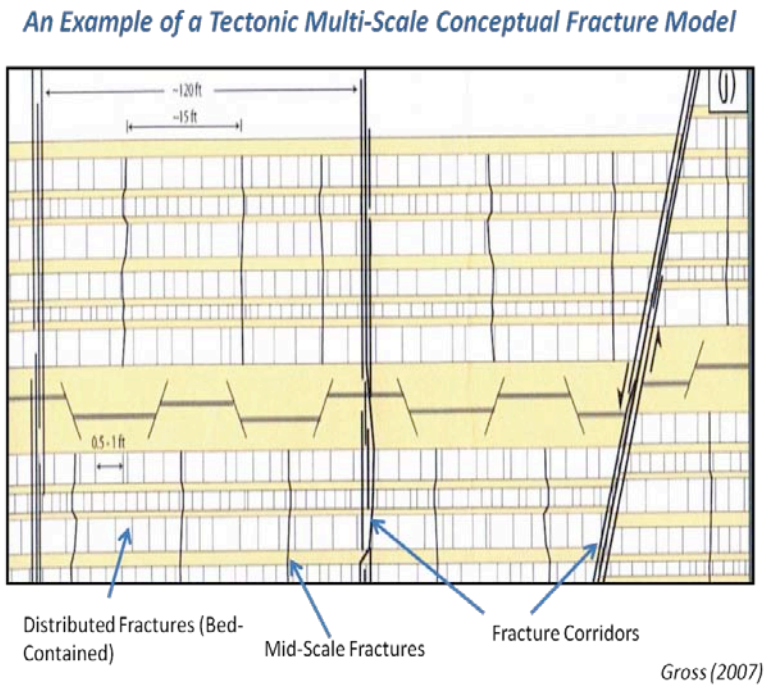

Fig. 9— Multi scale conceptual fracture model by Gross et al (2007)

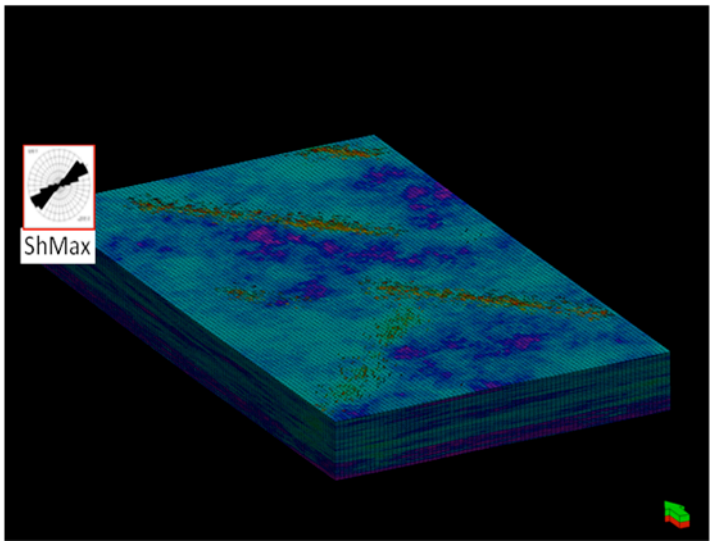

Fig. 10— Dual porosity simulation model highlighting the fracture corridors (red in color)

Full Vertical Communication vs Vertical Barriers. Sensitivity runs on two different geologic features (full vertical communication as well as vertical barriers via the bounding shale layers) are completed on Well A. **Table 2** shows the estimated ultimate recoverable (EUR) for the two cases. **Fig 11.** shows the pressure distribution of the two models after 30 years of production.

TABLE 2 – EUR COMPARISON FOR SINGLE WELL STUDY	
Simulation Scenario	EUR (MBO)
Full Vertical Communication	900
Vertical Barriers (Bounding Shales)	330

As illustrated in **Table 2** and **Fig 11**, degree of vertical communication is crucial in term of estimating the accurate reserves for this kind of reservoir and completion technique. Both field data and detail reservoir characterization imply that the bounding layers can contribute to production through either natural fracture networks or the hydraulic fractures.

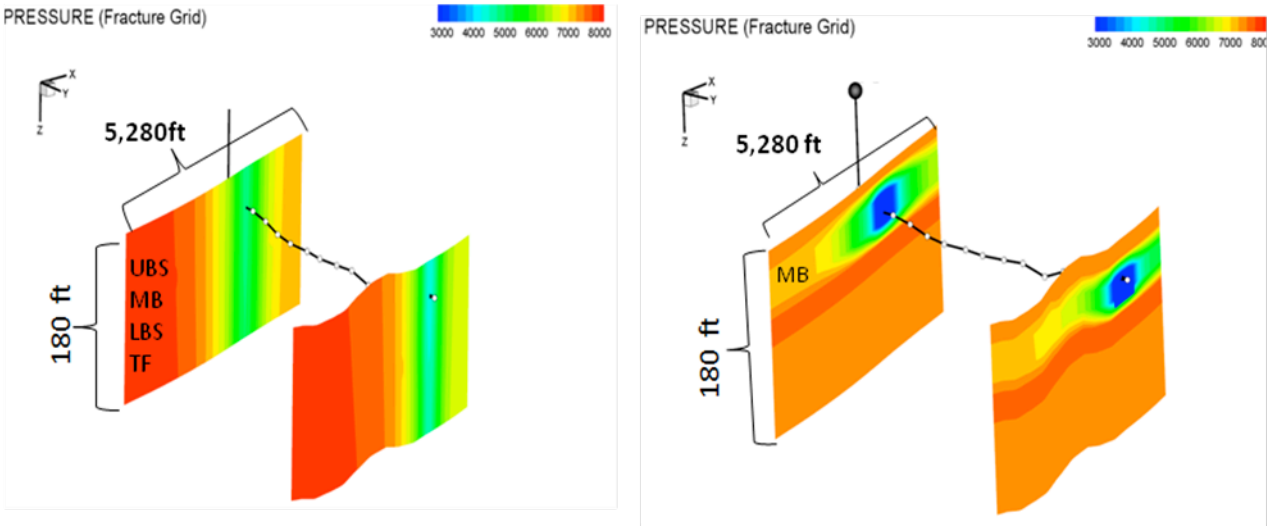

Fig. 11— Single Well Pressure Depletion Comparison

Conceptual Development Scenarios. Unconventional reservoirs similar to Bakken typically will need a large development program to efficiently drain the reserves. A conceptual development was performed on the simulation models to illustrate the sensitivity of the number of wells to the reservoir characterization. **Fig 12.** illustrates the pressure depletion for a development scenario of three Middle Bakken and Three Forks wells in the two extreme geologic scenarios (full vertical communication as well as vertical barriers via the shale units). **Table 3** shows the estimated total EUR for the drilling spacing units. The results suggest that the optimum number of wells is highly sensitive to the characterization of the reservoir, especially the degree of vertical communication.

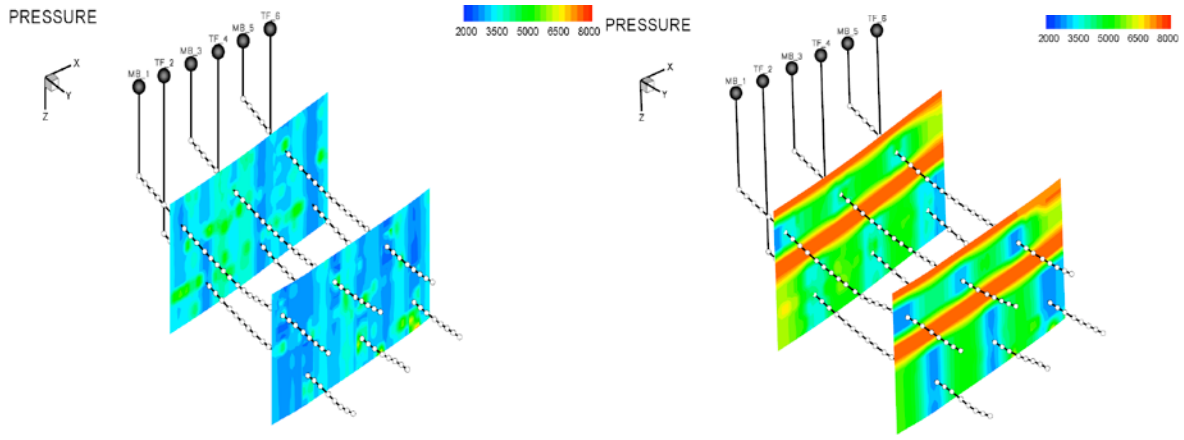

Fig. 12— Conceptual Development Pressure Depletion Comparison

TABLE 3 – EUR COMPARISON FOR CONCEPTUAL DEVELOPMENT		
Well Count	Geologic Scenario	Total EUR in Spacing Unit (MMBO)
3 Middle Bakken and 3 Three Forks	Single layer reservoir	2.5
5 Middle Bakken and 5 Three Forks	Single layer reservoir	3.5
3 Middle Bakken and 3 Three Forks	Vertically connected reservoir	4.0

A Calibrated Well Model. The result of geochemistry analysis in Well A was used to tune the transmissibility between layers in the simulation models. **Fig 13.** illustrates the pressure depletion and vertical permeability for Well A, which is calibrated to match the production allocation by layers measured by geochemistry. **Table 4** shows the EUR comparison between all cases. As expected, the calibrated well model's EUR is in between the two extreme geologic scenarios.

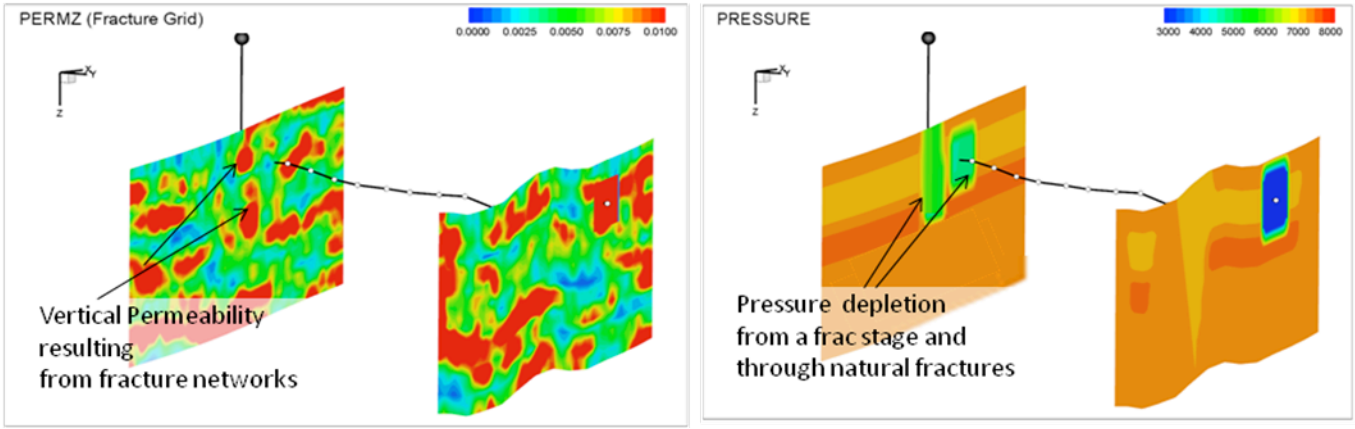

Fig. 13— Vertical Permeability and Pressure Depletion for A Calibrated Well Model

TABLE 4 – EUR COMPARISON FOR ALL CASES	
Scenario	EUR (MBO)
Full vertical connection	900
Single Layer	330
Calibrated Well Model	650

Production Decline Behavior

This section discusses the production behavior of the two simulated geologic scenarios and field examples. Kabir et al. (2010) evaluated various modern production analysis for unconventional and found that methods advocated by Valko and Lee (2010) offers excellent modern analysis techniques for long term performance forecasting in unconventional reservoirs. This study focused on the possibility of multi layer production in the Bakken and thus chose to utilize the work done by Fetkovich (1980) to address the multi layers production decline behaviors with respect to decline parameter, *b*-factor.

Hough and McClurg (2011) have shown in their work that the average *b*-factor in the Bakken can range from less than 1.0 to 4.0. This implies that the reservoir is in transient flow for a long period of time due to long planar fractures or multi-layered system. The geochemistry analyses and simulation have shown that Bakken may be in transient flow due to its multi-layerd production and long planar fractures.

Spivey et al. (2001) introduces the concept of the transient hyperbolic exponent, *b*. They inferred that a *b*-factor of more than 1.0 in unconventional reservoir or coal bed methane can be associated with commingled production from bounding layers. This paper uses the transient *b*-factor method to calculate the *b*-factor for the two simulated geologic scenarios and for field data. **Fig 14.** shows the calculated transient *b*-factor for the two simulated geologic scenarios and two field examples in the Bakken. The field examples late time *b*-factor lies in between the two extreme geologic scenarios. This observation may indicate that the two wells are producing from more than one layer. This observation is not limited to these two wells, more than 200 wells have shown a late time (more than 900 production days) *b*-factor in between 1.0 and 2.0. This decline behavior, geochemistry results, and detail fracture characterization models recommend a well in the Bakken system might be producing from more than one geologic unit.

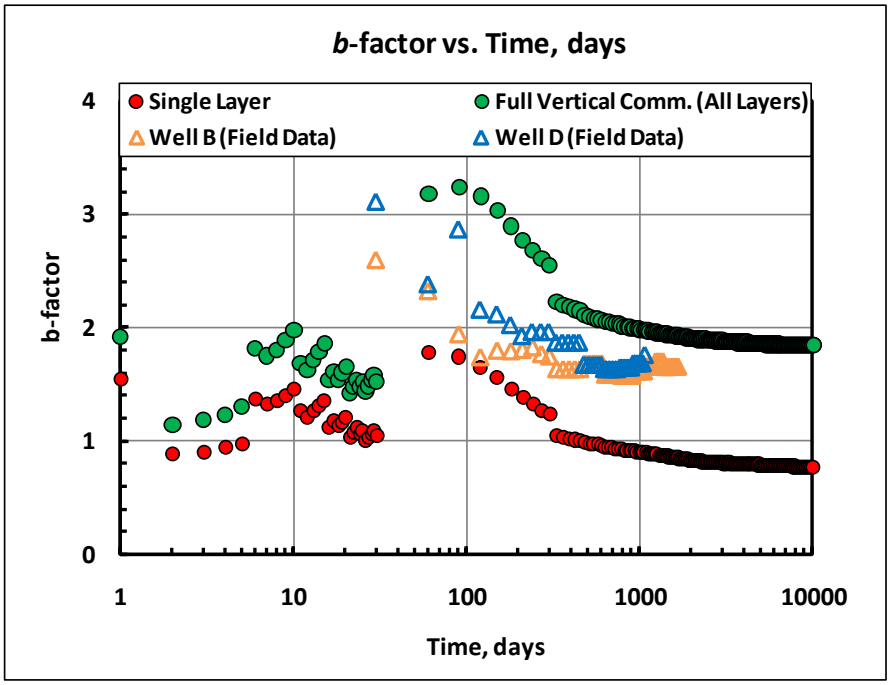

Fig. 14— *b*-factor Comparison for Simulated Data and Field Examples

Conclusion

- Field data in the Bakken suggest that layers within the Bakken system may communicate during stimulation and production.
- Geochemistry can be utilized to differentiate and allocate production between multiple horizons in the same petroleum system. The geochemistry results should complement any data that goes into the construction of reservoir simulation model.
- A detailed fracture network model or discreet fracture network (DFN) is needed in order to fully characterize vertical communication, optimize infill well development and understanding the full potential of the Bakken system.
- A simple observation of *b*-factor with time, field data and conceptual simulation response agrees with the geochemistry and the detailed DFN characterization.

Nomenclature

Roman

b = Arps decline parameter, dimensionless

C = Hydrocarbon chain

LP = Lodge Pole

LBS = Lower Bakken Shale Zone

MB = Middle Bakken Zone

TF = Three Forks Zone

UBS = Upper Bakken Shale Zone

Greek

$\delta^{13}C$ = C-13/C-12 isotopic ratio

Acknowledgements

The authors would like to thank Marathon Oil Corporation management, especially to Russ Buettner and Rohit Sinha for thoroughly reviewing the work and permission to publish this work. We would also like to acknowledge our peers from Bakken Asset Team and Upstream Technology for their reviews, comments and feedback. We are thankful for Sebastian Bayer, Jason Chen, Felipe Lozano and Stephen Buckner for their efforts in building the detail discreet fracture networks model, which is key in understanding the behavior of fracture reservoirs like the Bakken.

References

Bennett, B., Adams, J.A. and Lartner, S.R. 2009. Oil Fingerprinting for Production Allocation: Exploiting the Natural Variations in Fluid Properties Encountered In Heavy Oil and Oil Sand Reservoirs. Presented at CSPG CSEG CWLS Convention, Calgary, Alberta, Canada, 2009.

Bissada, K.K. et al. 1992. Geochemical Inversion – A Modern Approach to Inferring Source-Rock Identity from Characteristics of Accumulated Oil and Gas, American Association of Petroleum Geologist 21st Annual Convention Proceedings (Volume 1), p. 165-199

Cipolla, C., Lewis, R., Maxwell, S., and Mack, M. 2011. Appraising Unconventional Resource Plays: Separating Reservoir Quality from Completion Effectiveness, SPE paper 14677 presented at the International Petroleum Technology Conference, Bangkok, Thailand, 7-9 February.

Cipolla, C., Maxwell, S., and Mack, M. 2010. Reducing Exploration and Appraisal Risk in Low-Permeability Reservoirs Using Microseismic Fracture Mapping, SPE paper 137467 presented at the Canadian Unconventional Resources and International Petroleum Conference, Calgary, Canada, 19-21October.

Ejofodomi, E., et al. 2011. Integrating All Available Data to Improve Production in the Marcellus Shale, SPE paper 144321 presented at the SPE North American Unconventional Gas Conference and Exhibition, The Woodlands, Texas, USA, 14-16 June.

Fetkovich, M. J.: "Decline Curve Analysis Using Type Curves," *JPT* (June 1980) 1065-77.

Gross, M. R., and Y. Eyal, 2007, Through going Fractures in Layered Carbonate Rocks: Geological Society of America Bulletin, v. 119, p. 1387－1404.

Hough, E.V., McClurg, T., 2011, Impact of Geologic Variation and Completion Type in the US Bakken Oil Shale Play Using Decline Curve Analysis and Transient Flow Character, Article #40857(2011) presented at AAPG International Conference and Exhibition, Milan, Italy, October 23-26.

Kabir, C. S., Rasdi, F., and Igboalisi, B. 2010. Analyzing Production Data From Tight Oil Wells, SPE paper 137414 presented at the SPE/CSUG Canadian Unconventional Resources and International Petroleum Conference, Calgary, Alberta, Canada, 10–21 October.

Mullen, M., et al. 2010. Does the Presence of Natural Fractures Have an Impact on Production? A Case Study From the Middle Bakken Dolomite, North Dakota, SPE paper 135319 presented at the SPE Annual Technical Conference, Florence, Italy, 19-22 September.

McCaffrey, M.A., Legarre, H. A., and Johnson, S.J. 1996. Using Biomarkers to Improve Heavy Oil Reservoir Management: An Example from the Cymric Field, Kern County, California. American Association of Petroleum Geologist Bulletin 80, 904-919.

McCaffrey, M.A., et al. 2010. Geochemical Allocation of Commingled Oil Production and/or Commingled Gas Production from 2-6 Pay Zones. Article #90110(2010) presented at AAPG Hedberg Conference, Vail, Colorado, June 8-11.

MsCaffrey, M.A., et al. 2011. Geochemical Allocation of Commingled Oil Production or Commingled Gas Production. SPE paper 144618 presented at the SPE Western North American Regional Meeting, Anchorage, Alaska, May 7-11.

McCaffrey, M.A. et al.: "Oil Fingerprinting Dramatically Reduces Production Allocation Costs." *World Oil* (March 2012) 55-59.

Pitman, J.K. et al. 2001. Diagenesis and Fracture Development in the Bakken Formation, Williston Basin: Implication of Reservoir Quality in the Middle Member. U.S Geological Survey Professional Paper 1653: 1-17

Rasdi, F. and Chu, L. 2012. Diagnosing Fracture Network Pattern and Flow Regime Aids Production Performance Analysis in Unconventional Oil Reservoirs, SPE paper 151623 presented at the SPE/EAGE Unconventional Resources Conference and Exhibition, Vienna, Austria, 20-22 March.

Spivey, J. P., Frantz, J.H., Williamson, J.R., and Sawyer, W.K. 2001. Application of the Transient Hyperbolic Exponent, SPE paper 71038 presented at the SPE Rocky Mountain Petroleum Technology Conference, Keystone, Colorado, USA, 21-23 May.

U.S. Geological Survey. 2008. Assessment of Undiscovered Oil Resources in The Devonian-Mississippian Bakken Formation, Williston Basin Province, Montana and North Dakota: USGS Fact Sheet 2008-3021: http://pubs.usgs.gov/fs/2008/3021/pdf/FS08-3021_508.pdf

Valko, P.P. 2009. Assigning value to Simulation in the Barnett Shale: A Simultaneous Analysis of 7,000 plus Production Histories and Well Completion Records. SPE Paper 119369 presented at the SPE Hydraulic fracturing Technology Conference., The Woodlands, TX, 19-21 January.

Appendix A – Production Allocation Method

This appendix explains the method to calculate and allocate production by geologic members. The method was originally proposed by McCaffrey et al. (1996, 2010). In this example, a well producing in the Three Forks was analyzed. **Table 5** shows the concentration and $\delta^{13}C$ for the Three Forks producers.

Table 5—Concentration and δ13C isotopic value data for an Upper Three Forks commingled produced oil example									
End Member	**% Saturate**	**% Aromatic**	**% NSO**	**% Asphaltene**	**δ^{13}C Saturate**	**δ^{13}C Aromatic**	**δ^{13}C NSO**	**δ^{13}C Asphaltene**	**δ^{13}C Whole Oil**
Lodgepole (LP)	$\%S_{LP}$	$\%A_{LP}$	$\%N_{LP}$	$\%AS_{LP}$	$\delta^{13}C\ S_{LP}$	$\delta^{13}C\ A_{LP}$	$\delta^{13}C\ N_{LP}$	$\delta^{13}C\ AS_{LP}$	$\delta^{13}C\ W_{LP}$
Upper Bakken Shale (UBS)	$\%S_{UBS}$	$\%A_{UBS}$	$\%N_{UBS}$	$\%AS_{UBS}$	$\delta^{13}C\ S_{UBS}$	$\delta^{13}C\ A_{UBS}$	$\delta^{13}C\ N_{UBS}$	$\delta^{13}C\ AS_{UBS}$	$\delta^{13}C\ W_{UBS}$
Middle Bakken (MB)	$\%S_{MB}$	$\%A_{MB}$	$\%N_{MB}$	$\%AS_{MB}$	$\delta^{13}C\ S_{MB}$	$\delta^{13}C\ A_{MB}$	$\delta^{13}C\ N_{MB}$	$\delta^{13}C\ AS_{MB}$	$\delta^{13}C\ W_{MB}$
Lower Bakken Shale (LBS)	$\%S_{LBS}$	$\%A_{LBS}$	$\%N_{LBS}$	$\%AS_{LBS}$	$\delta^{13}C\ S_{LBS}$	$\delta^{13}C\ A_{LBS}$	$\delta^{13}C\ N_{LBS}$	$\delta^{13}C\ AS_{LBS}$	$\delta^{13}C\ W_{LBS}$
Upper Three Forks (UTF)	$\%S_{UTF}$	$\%A_{UTF}$	$\%N_{UTF}$	$\%AS_{UTF}$	$\delta^{13}C\ S_{UTF}$	$\delta^{13}C\ A_{UTF}$	$\delta^{13}C\ N_{UTF}$	$\delta^{13}C\ AS_{UTF}$	$\delta^{13}C\ W_{UTF}$
Commingled Produced Oil (CPO)	$\%S_{CPO}$	$\%A_{CPO}$	$\%N_{CPO}$	$\%AS_{CPO}$	$\delta^{13}C\ S_{CPO}$	$\delta^{13}C\ A_{CPO}$	$\delta^{13}C\ N_{CPO}$	$\delta^{13}C\ AS_{CPO}$	$\delta^{13}C\ W_{CPO}$

Equations measuring the mixing of component concentrations and δ^{13}C isotope value are shown below.

Saturate carbon isotopes:

$$\%S_{LP} * \left((\delta 13C\ S_{CPO}) - (\delta 13C\ S_{LP})\right) * frac(LP) + \%S_{UBS} * \left((\delta 13C\ S_{CPO}) - (\delta 13C\ S_{UBS})\right) * frac(UBS) + \%S_{MB} * \left((\delta 13C\ S_{CPO}) - (\delta 13C\ S_{MB})\right) * frac(MB)$$
$$\ldots \%S_{LBS} * \left((\delta 13C\ S_{CPO}) - (\delta 13C\ S_{LBS})\right) * frac(LBS) + \%S_{UTF} * \left((\delta 13C\ S_{CPO}) - (\delta 13C\ S_{UTF})\right) * frac(UTF) + E_1 = 0$$

Aromatic carbon isotopes:

$$\%A_{LP} * \left((\delta 13C\ A_{CPO}) - (\delta 13C\ A_{LP})\right) * frac(LP) + \%A_{UBS} * \left((\delta 13C\ A_{CPO}) - (\delta 13C\ A_{UBS})\right) * frac(UBS) + \%A_{MB} * \left((\delta 13C\ A_{CPO}) - (\delta 13C\ A_{MB})\right) * frac(MB)$$
$$\ldots \%A_{LBS} * \left((\delta 13C\ A_{CPO}) - (\delta 13C\ A_{LBS})\right) * frac(LBS) + \%A_{UTF} * \left((\delta 13C\ A_{CPO}) - (\delta 13C\ A_{UTF})\right) * frac(UTF) + E_2 = 0$$

NSO carbon isotopes:

$$\%N_{LP} * \left((\delta 13C\ N_{CPO}) - (\delta 13C\ N_{LP})\right) * frac(LP) + \%N_{UBS} * \left((\delta 13C\ N_{CPO}) - (\delta 13C\ N_{UBS})\right) * frac(UBS) + \%N_{MB} * \left((\delta 13C\ N_{CPO}) - (\delta 13C\ N_{MB})\right) * frac(MB)$$
$$\ldots + \%N_{LBS} * \left((\delta 13C\ N_{CPO}) - (\delta 13C\ N_{LBS})\right) * frac(LBS) + \%N_{UTF} * \left((\delta 13C\ N_{CPO}) - (\delta 13C\ N_{UTF})\right) * frac(UTF) + E_3 = 0$$

Asphaltene carbon isotopes:

$$\%AS_{LP} * \left((\delta 13C\ AS_{CPO}) - (\delta 13C\ AS_{LP})\right) * frac(LP) + \%AS_{UBS} * \left((\delta 13C\ AS_{CPO}) - (\delta 13C\ AS_{UBS})\right) * frac(UBS) + \%AS_{MB} * \left((\delta 13C\ AS_{CPO}) - (\delta 13C\ AS_{MB})\right) * frac(MB)$$
$$\ldots + \%AS_{LBS} * \left((\delta 13C\ AS_{CPO}) - (\delta 13C\ AS_{LBS})\right) * frac(LBS) + \%AS_{UTF} * \left((\delta 13C\ AS_{CPO}) - (\delta 13C\ AS_{UTF})\right) * frac(UTF) + E_4 = 0$$

Whole oil carbon isotopes:

$$\%W_{LP} * \left((\delta 13C\ W_{CPO}) - (\delta 13C\ W_{LP})\right) * frac(LP) + \%W_{UBS} * \left((\delta 13C\ W_{CPO}) - (\delta 13C\ W_{UBS})\right) * frac(UBS) + \%W_{MB} * \left((\delta 13C\ W_{CPO}) - (\delta 13C\ W_{MB})\right) * frac(MB)$$
$$\ldots + \%W_{LBS} * \left((\delta 13C\ W_{CPO}) - (\delta 13C\ W_{LBS})\right) * frac(LBS) + \%W_{UTF} * \left((\delta 13C\ W_{CPO}) - (\delta 13C\ W_{UTF})\right) * frac(UTF) + E_5 = 0$$

Fraction sum equal to 1:

$$frac(LP) + frac(UBS) + frac(MB) + frac(LBS) + frac(UTF) + E_6 = 1$$

These equations form the matrices used to solve for percent contribution from each end member using linear regression. One can utilize the following formula to simultaneously solve the system of equations:

$$A = [X^T X]^{-1} X^T Y$$

Where:

A (6x1 matrix) = Percentage contribution from each stratigraphic zone in the produced oil sample

X (6x6 matrix) = End member saturate and aromatic concentration and δ^{13}C saturate and aromatic value equations which can create a produced oil mixture that also incorporates error terms

Y (6x1 matrix) = Produced oil saturate and aromatic concentration and δ^{13}C saturate and aromatic values

$$X = \begin{bmatrix} \%S_{LP} * (\delta^{13}C\ S_{CPO} - \delta^{13}C\ S_{LP}) & \%S_{UBS} * (\delta^{13}C\ S_{CPO} - \delta^{13}C\ S_{UBS}) & \%S_{MB} * (\delta^{13}C\ S_{CPO} - \delta^{13}C\ S_{MB}) & \%S_{LBS} * (\delta^{13}C\ S_{CPO} - \delta^{13}C\ S_{LBS}) & \%S_{UTF} * (\delta^{13}C\ S_{CPO} - \delta^{13}C\ S_{UTF}) & \overline{E}_1 \\ \%A_{LP} * (\delta^{13}C\ A_{CPO} - \delta^{13}C\ A_{LP}) & \%A_{UBS} * (\delta^{13}C\ A_{CPO} - \delta^{13}C\ A_{UBS}) & \%A_{MB} * (\delta^{13}C\ A_{CPO} - \delta^{13}C\ A_{MB}) & \%A_{LBS} * (\delta^{13}C\ A_{CPO} - \delta^{13}C\ A_{LBS}) & \%A_{UTF} * (\delta^{13}C\ A_{CPO} - \delta^{13}C\ A_{UTF}) & \overline{E}_2 \\ \%N_{LP} * (\delta^{13}C\ N_{CPO} - \delta^{13}C\ N_{LP}) & \%N_{UBS} * (\delta^{13}C\ N_{CPO} - \delta^{13}C\ N_{UBS}) & \%N_{MB} * (\delta^{13}C\ N_{CPO} - \delta^{13}C\ N_{MB}) & \%N_{LBS} * (\delta^{13}C\ N_{CPO} - \delta^{13}C\ N_{LBS}) & \%N_{UTF} * (\delta^{13}C\ N_{CPO} - \delta^{13}C\ N_{UTF}) & \overline{E}_3 \\ \%AS_{LP} * (\delta^{13}C\ AS_{CPO} - \delta^{13}C\ AS_{LP}) & \%AS_{UBS} * (\delta^{13}C\ AS_{CPO} - \delta^{13}C\ AS_{UBS}) & \%AS_{MB} * (\delta^{13}C\ AS_{CPO} - \delta^{13}C\ AS_{MB}) & \%AS_{LBS} * (\delta^{13}C\ AS_{CPO} - \delta^{13}C\ AS_{LBS}) & \%AS_{UTF} * (\delta^{13}C\ AS_{CPO} - \delta^{13}C\ AS_{UTF}) & \overline{E}_4 \\ \%W_{LP} * (\delta^{13}C\ W_{CPO} - \delta^{13}C\ W_{LP}) & \%W_{UBS} * (\delta^{13}C\ W_{CPO} - \delta^{13}C\ W_{UBS}) & \%W_{MB} * (\delta^{13}C\ W_{CPO} - \delta^{13}C\ W_{MB}) & \%W_{LBS} * (\delta^{13}C\ W_{CPO} - \delta^{13}C\ W_{LBS}) & \%W_{UTF} * (\delta^{13}C\ W_{CPO} - \delta^{13}C\ W_{UTF}) & \overline{E}_5 \\ 1 & 1 & 1 & 1 & 1 & \overline{E}_6 \end{bmatrix}$$

$$Y = \begin{bmatrix} 0 \\ 0 \\ 0 \\ 0 \\ 0 \\ 1 \end{bmatrix}$$

$$A = \begin{bmatrix} frac(LP) \\ frac(UBS) \\ frac(MB) \\ frac(LBS) \\ frac(UTF) \\ 0 \end{bmatrix}$$

Associated error for each equation used to solve for Least Squares Error:

$$\overline{E}_1 = 0 - [\%S_{LP} * \left((\delta 13C\ S_{CPO}) - (\delta 13C\ S_{LP})\right) * frac(LP) + \%S_{UBS} * \left((\delta 13C\ S_{CPO}) - (\delta 13C\ S_{UBS})\right) * frac(UBS)$$
$$\ldots + \%S_{MB} * \left((\delta 13C\ S_{CPO}) - (\delta 13C\ S_{MB})\right) * frac(MB) + \%S_{LBS} * \left((\delta 13C\ S_{CPO}) - (\delta 13C\ S_{LBS})\right) * frac(LBS) + \%S_{UTF} * \left((\delta 13C\ S_{CPO}) - (\delta 13C\ S_{UTF})\right) * frac(UTF)]$$

$$\overline{E}_2 = 0 - [\%A_{LP} * \left((\delta 13C\ A_{CPO}) - (\delta 13C\ A_{LP})\right) * frac(LP) + \%A_{UBS} * \left((\delta 13C\ A_{CPO}) - (\delta 13C\ A_{UBS})\right) * frac(UBS)$$
$$\ldots + \%A_{MB} * \left((\delta 13C\ A_{CPO}) - (\delta 13C\ A_{MB})\right) * frac(MB) + \%A_{LBS} * \left((\delta 13C\ A_{CPO}) - (\delta 13C\ A_{LBS})\right) * frac(LBS) + \%A_{UTF} * \left((\delta 13C\ A_{CPO}) - (\delta 13C\ A_{UTF})\right) * frac(UTF)]$$

$$\overline{E}_3 = 0 - [\%N_{LP} * \left((\delta 13C\ N_{CPO}) - (\delta 13C\ N_{LP})\right) * \mathrm{frac(LP)} + \%N_{UBS} * \left((\delta 13C\ N_{CPO}) - (\delta 13C\ N_{UBS})\right) * \mathrm{frac(UBS)}$$
$$\ldots + \%N_{MB} * \left((\delta 13C\ N_{CPO}) - (\delta 13C\ N_{MB})\right) * \mathrm{frac(MB)} + \%N_{LBS} * \left((\delta 13C\ N_{CPO}) - (\delta 13C\ N_{LBS})\right) * \mathrm{frac(LBS)} + \%N_{UTF} * \left((\delta 13C\ N_{CPO}) - (\delta 13C\ N_{UTF})\right) * \mathrm{frac(UTF)}]$$

$$\overline{E}_4 = 0 - [\%AS_{LP} * \left((\delta 13C\ AS_{CPO}) - (\delta 13C\ AS_{LP})\right) * \mathrm{frac(LP)} + \%AS_{UBS} * \left((\delta 13C\ AS_{CPO}) - (\delta 13C\ AS_{UBS})\right) * \mathrm{frac(UBS)}$$
$$\ldots + \%AS_{MB} * \left((\delta 13C\ AS_{CPO}) - (\delta 13C\ AS_{MB})\right) * \mathrm{frac(MB)} + \%AS_{LBS} * \left((\delta 13C\ AS_{CPO}) - (\delta 13C\ AS_{LBS})\right) * \mathrm{frac(LBS)}$$
$$\ldots + \%AS_{UTF} * \left((\delta 13C\ AS_{CPO}) - (\delta 13C\ AS_{UTF})\right) * \mathrm{frac(UTF)}]$$

$$\overline{E}_5 = 0 - [\%W_{LP} * \left((\delta 13C\ W_{CPO}) - (\delta 13C\ W_{LP})\right) * frac(LP) + \%W_{UBS} * \left((\delta 13C\ W_{CPO}) - (\delta 13C\ W_{UBS})\right) * frac(UBS)$$
$$\ldots + \%W_{MB} * \left((\delta 13C\ W_{CPO}) - (\delta 13C\ W_{MB})\right) * frac(MB) + \%W_{LBS} * \left((\delta 13C\ W_{CPO}) - (\delta 13C\ W_{LBS})\right) * frac(LBS)$$
$$\ldots + \%W_{UTF} * \left((\delta 13C\ W_{CPO}) - (\delta 13C\ W_{UTF})\right) * frac(UTF)]$$

$$\overline{E}_6 = 1 - [\ frac(LP) + frac(UBS) + frac(MB) + frac(LBS) + frac(UTF)\ ]$$

Where:

$\overline{E}_n$ = Smallest associated error for each equation in a system of equations

E_n = Associated error for each equation in a system of equations attributable to a single possible solution

These equations form the matrices used to solve for minimum sum of least squares error using linear regression:

$$\begin{bmatrix} \overline{E}_1 \\ \overline{E}_2 \\ \overline{E}_3 \\ \overline{E}_4 \\ \overline{E}_5 \\ \overline{E}_6 \end{bmatrix} = \begin{bmatrix} 0 \\ 0 \\ 0 \\ 0 \\ 0 \\ 1 \end{bmatrix} - \begin{bmatrix} \%S_{LP} * (\delta^{13}C\ S_{CPO} - \delta^{13}C\ S_{LP}) & \%S_{UBS} * (\delta^{13}C\ S_{CPO} - \delta^{13}C\ S_{UBS}) & \%S_{MB} * (\delta^{13}C\ S_{CPO} - \delta^{13}C\ S_{MB}) & \%S_{LBS} * (\delta^{13}C\ S_{CPO} - \delta^{13}C\ S_{LBS}) & \%S_{UTF} * (\delta^{13}C\ S_{CPO} - \delta^{13}C\ S_{UTF}) \\ \%A_{LP} * (\delta^{13}C\ A_{CPO} - \delta^{13}C\ A_{LP}) & \%A_{UBS} * (\delta^{13}C\ A_{CPO} - \delta^{13}C\ A_{UBS}) & \%A_{MB} * (\delta^{13}C\ A_{CPO} - \delta^{13}C\ A_{MB}) & \%A_{LBS} * (\delta^{13}C\ A_{CPO} - \delta^{13}C\ A_{LBS}) & \%A_{UTF} * (\delta^{13}C\ A_{CPO} - \delta^{13}C\ A_{UTF}) \\ \%N_{LP} * (\delta^{13}C\ N_{CPO} - \delta^{13}C\ N_{LP}) & \%N_{UBS} * (\delta^{13}C\ N_{CPO} - \delta^{13}C\ N_{UBS}) & \%N_{MB} * (\delta^{13}C\ N_{CPO} - \delta^{13}C\ N_{MB}) & \%N_{LBS} * (\delta^{13}C\ N_{CPO} - \delta^{13}C\ N_{LBS}) & \%N_{UTF} * (\delta^{13}C\ N_{CPO} - \delta^{13}C\ N_{UTF}) \\ \%AS_{LP} * (\delta^{13}C\ AS_{CPO} - \delta^{13}C\ AS_{LP}) & \%AS_{UBS} * (\delta^{13}C\ AS_{CPO} - \delta^{13}C\ AS_{UBS}) & \%AS_{MB} * (\delta^{13}C\ AS_{CPO} - \delta^{13}C\ AS_{MB}) & \%AS_{LBS} * (\delta^{13}C\ AS_{CPO} - \delta^{13}C\ AS_{LBS}) & \%AS_{UTF} * (\delta^{13}C\ AS_{CPO} - \delta^{13}C\ AS_{UTF}) \\ \%W_{LP} * (\delta^{13}C\ W_{CPO} - \delta^{13}C\ W_{LP}) & \%W_{UBS} * (\delta^{13}C\ W_{CPO} - \delta^{13}C\ W_{UBS}) & \%W_{MB} * (\delta^{13}C\ W_{CPO} - \delta^{13}C\ W_{MB}) & \%W_{LBS} * (\delta^{13}C\ W_{CPO} - \delta^{13}C\ W_{LBS}) & \%W_{UTF} * (\delta^{13}C\ W_{CPO} - \delta^{13}C\ W_{UTF}) \\ 1 & 1 & 1 & 1 & 1 \end{bmatrix} \begin{bmatrix} frac(LP) \\ frac(UBS) \\ frac(MB) \\ frac(LBS) \\ frac(UTF) \end{bmatrix}$$

Definition of Least Squares Error:

$$\overline{\varepsilon}^2 = \overline{E}_1^2 + \overline{E}_2^2 + \overline{E}_3^2 + \overline{E}_4^2 + \overline{E}_5^2$$

Where:

$$\overline{\varepsilon}^2 = \overline{E}_1^2 + \overline{E}_2^2 + \overline{E}_3^2 + \overline{E}_4^2 + \overline{E}_5^2 < \varepsilon^2 = E_1^2 + E_2^2 + E_3^2 + E_4^2 + E_5^2$$

$$\overline{\varepsilon} < \varepsilon$$

$$\overline{\sigma} = \frac{\overline{\varepsilon}}{(n-m)}$$

Where:

$\overline{E}_n$ = Smallest associated error for each equation in a system of equations

$\overline{\varepsilon}$ = Least squares error

E_n = Associated error for each equation in a system of equations attributable to a single possible solution

ε = Squares error attributable to another possible solution

$\overline{\sigma}$ = Standard deviation of Least Squares Error

n = Number of variables

m = Number of end members